

Experimental Analysis of Flow Fields inside Intake Heads of a Vacuum Cleaner

Daichin

*Institute of Applied Mathematics and Mechanics, Shang Hai University,
Shang hai, 200072, China*

Sang-Joon Lee*

*Department of Mechanical Engineering,
Pohang University of Science and Technology, Pohang 790-784, Korea*

The flow structure inside the intake head greatly affects the working efficiency of a vacuum cleaner such as suction power and aero-acoustic noise. In this study, the flow inside intake heads of a vacuum cleaner was investigated using qualitative flow visualization and quantitative PIV (Particle Image Velocimetry) techniques. The aerodynamic power, suction efficiency and noise level of the intake heads were also measured. In order to improve the performance of the vacuum cleaner, inner structure of the flow paths of the intake head, such as trench height and shape of connection chamber were modified. The flow structures of modified intake heads were compared with that of the original intake head. The aero-acoustic noise caused by flow separation was reduced and the suction efficiency was also changed due to flow path modification of intake head. In this paper, the variations of flow fields for different intake heads are presented and discussed together with results of aerodynamic power, suction efficiency and noise level.

Key Words : Vacuum Cleaner, Intake Head, Flow Structure, Suction Efficiency

1. Introduction

Vacuum cleaners have been used as an efficient laborsaving home appliance for cleaning up a room. It is composed of two main parts: the mechanical part generating suction pressure by a vacuum working fan (VWF), and the intake part used to collect dusts. These two parts usually connected by a tube or a flexible hose. A vacuum cleaner collects dusts, dirt and debris with strong air stream caused by sub-atmospheric pressure difference. Customers usually prefer a vacuum cleaner having a strong suction power. To satisfy

such demands, it is necessary to increase the electric motor capacity for enhancing the suction power of dusts removal. However, aero-acoustic noise level is another important factor used for evaluating the quality of a vacuum cleaner. Generally, acoustic noise generated from a vacuum cleaner results from following mechanisms: (1) airborne noise caused by air flow separation inside the device, (2) vibration caused by unbalance rotating of fan and motor, blower and vacuum working fan, and (3) mechanical friction. The most annoying one is the airborne noise caused by airflow separation and turbulence.

Several researches on vacuum cleaners have been reported. However, most of them are mainly concerned with the methodology to improve the suction power and control the acoustic noise emission. Bentouati et al. (1999) designed single-phase and three-phase permanent magnet brushless DC motors for retrofitting to a vacuum cleaner. The 3-phase brushless DC motor im-

* Corresponding Author,

E-mail : sjlee@postech.ac.kr

TEL : +82-54-279-2169; **FAX :** +82-54-279-3199

Department of Mechanical Engineering, Pohang University of Science and Technology, Pohang 790-784, Korea. (Manuscript **Received** August 26, 2004; **Revised** January 10, 2005)

proves the efficiency about 25–30% and decreases the noise level about 8dB compared with that of the universal motor. Omori and Uzawa (1997) developed a vacuum cleaner with brush that is efficient in removing adhesive particles.

For acoustic noise reduction, Sarbu and Kraft (1996) used sound intensity methods to redesign a vacuum cleaner and reduced the sound power level by 5.7dB. Brungart and Lanchle (2001) reduced noise level of a handheld vacuum cleaner by modifying the casing of vacuum fan. They found that the noise radiated from a vacuum cleaner was dominated by aerodynamic sources with the tone at the blade passing frequency (BPF) of the fan.

As far as the authors recognize, there is no literature investigating the internal flow structure inside a vacuum cleaner, especially the intake flow at the intake head. It is desirable to understand the flow structure and to control the intake flow effectively for reducing acoustic-noise and improving the suction efficiency.

The main objective of this study is to investigate the flow structure inside the intake head of a household vacuum cleaner in detail. The experimental results obtained by flow visualization and PIV (Particle Image Velocimetry) measurements are discussed together with the results of pressure and acoustic noise level.

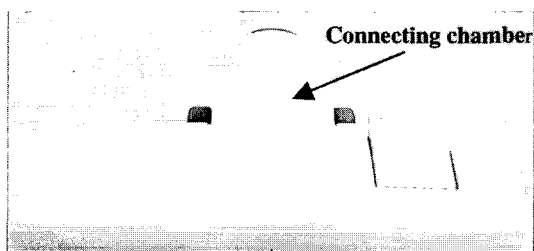
2. Experimental Apparatus and Methods

2.1 Intake heads of vacuum cleaner

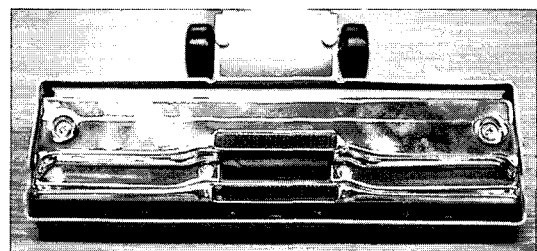
In the present study, an intake head of a commercial household vacuum cleaner was used as a

reference model. The top and side views of the original intake head are shown in Fig. 1. In order to improve the dust-collection ability and reduce acoustic-noise level of the vacuum cleaner, the internal geometry of the intake head was modified. The inclination angle of bottom surface of two main side trenches of the original intake head is about 6.8° . At first, a small plate of 0.8 mm thick was attached on inner half of bottom surface of two side trenches as shown in Fig. 2(a), decreasing the inclination angle to 5° . The inclination angle was reduced in the consideration to decrease the possibility of flow separation and energy dissipation at inlet corner of suction hole and trench surface. Fig. 2(a) shows bottom view and transect of the modified trenches linked to the central suction hole. Fig. 3(a) shows the vertical section of right half trench and suction hole. The coordinate system is defined in Fig. 2(a), 3(a) and 4.

The intake head is connected to the hand-holding suction pipe by a rectangular connection chamber. Therefore, the flow passing through the rectangular chamber into a circular suction pipe will cause friction loss and a sudden pressure drop. This results from the increased turbulence and vortex motion in the separated flow region, which is closely related with the decrease of suction power and increase of flow-induced noise. In order to reduce this kind of adverse aspects, plaster was filled inside the rectangular connection chamber to make a streamlined contour. Therefore, the sudden contraction at inlet of circular suction pipe is changed to a smooth contraction varying gradually from concave to convex wall. The contraction ratio which is defined

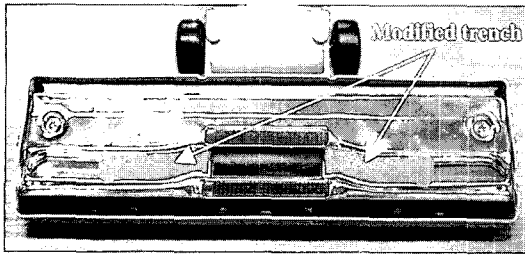


(a) Top view

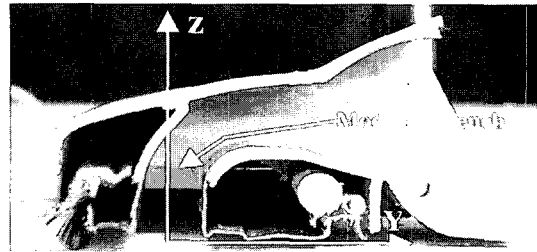


(b) Bottom view

Fig. 1 Top and bottom view of the original intake head

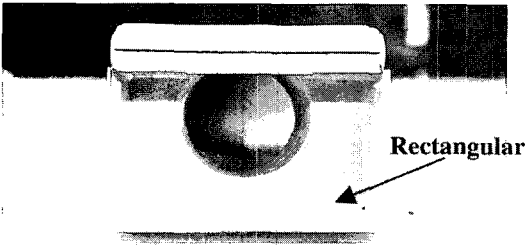


Bottom view

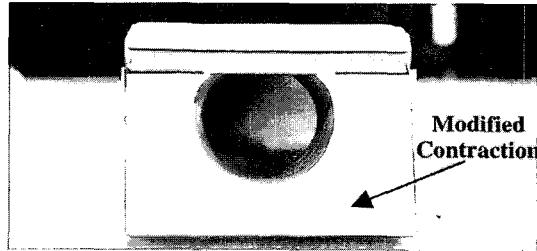


Side view

(a) Trench height modification



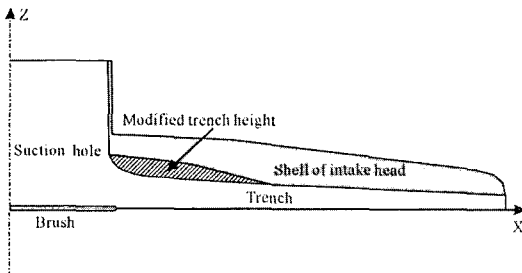
Bottom view



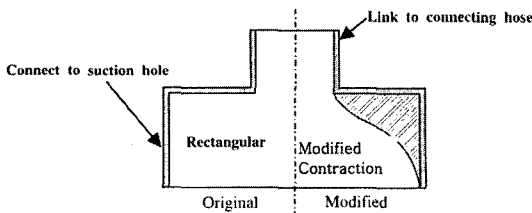
Side view

(b) Connection chamber modification

Fig. 2 Photographs of airflow paths of modified intake heads



(a) Trench height modification



(b) Connection chamber modification

Fig. 3 Schematic diagram of trench height modification and modified connection chamber

as the area ratio of rectangular entrance to the circular-shaped exit of connecting chamber is about 2.8. Fig. 2(b) and 3(b) show the original rectangular connection chamber and the modified version with smooth contraction.

2.2 Flow visualization and PIV measurements

Fig. 4 shows the schematic diagram of experimental set-up for flow visualization and PIV measurements. A vacuum cleaner intake head was placed on the bottom surface of a transparent rectangular chamber of $70 \times 70 \times 40 \text{ cm}^3$ in size. The time series of tracing particle movement were taken by a CCD camera beneath the chamber.

During the flow visualization experiments, for each intake head, the particle images were captured by a high-speed CCD camera (SpeedCam 512) with frame rate of 500 frames/sec at spatial resolution of 512×512 pixels for 2 seconds. The test section was illuminated by a halogen lamp (300 watt). Because the two side trenches are symmetric with respect to the central suction hole, the whole central suction area and a part of right trench were visualized. Before the experiment, polystyrene particles of $100 \sim 200 \mu\text{m}$ in diameter are evenly spread out on the bottom surface of the rectangular chamber to simulate the dusts particles.

By replaying the recorded movies slowly, we

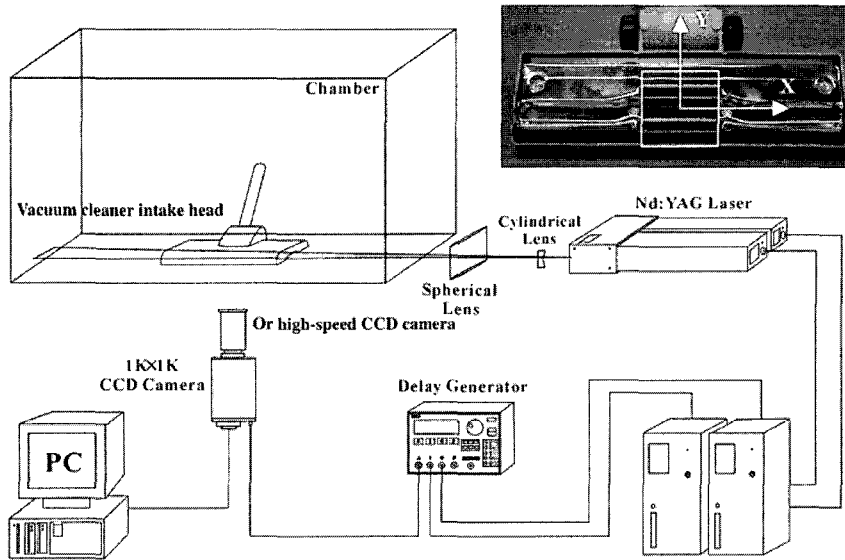


Fig. 4 Schematic diagram of experimental set-up for flow visualization and PIV measurement

can see clearly the temporal evolution of particles sucked into the suction hole. We define the total elapse time as the time duration between the start-up of a vacuum cleaner and the moment of the vacuum cleaner becoming a steady state. Since the suction efficiency is different for each tested intake head, total elapse time also depends on the flow path of intake head.

The velocity fields just beneath the central suction hole of the intake head were measured using a PIV system. A thin laser light sheet was made by passing a laser beam through cylindrical lenses to illuminate the testing section from the side of intake head. Because the sidewall of the intake head is not transparent, the laser light could not pass through it directly. The laser light sheet was arranged to pass through the small gap between the side trench and bottom plate of the test chamber. The test section for the PIV measurements at the entrance of suction is shown in Fig. 4 and testing area was $50 \times 50 \text{ mm}^2$.

The PIV system used in this study consists of a dual-head Nd: YAG laser, a Kodak CCD camera with a resolution of 1008×1018 pixels, a frame grabber, a delay generator and a PC. The delay generator was used to synchronize the laser and CCD camera. The time interval between two laser pulses was $18.0 \mu\text{s}$. The maximum energy of

the Nd: YAG laser is about 25 mJ per pulse with a 10 Hz repetition rate. Atomized olive oil particles with an average diameter of $2 \sim 3 \mu\text{m}$ were used as seeding particles. The vacuum cleaner was operated at the maximum power mode during the experiments.

2.3 Suction efficiency and noise level measurements

In order to compare quantitatively the suction efficiency of vacuum cleaner with modifying the original intake heads, the aerodynamic power, suction efficiency and noise level were measured. The aerodynamic power and suction efficiency of the vacuum cleaner were tested using a vacuum chamber, designed according to the Korean Standards (KS) and Japanese Industrial Standard (JIS) test regulations for vacuum cleaners. Fig. 5 shows the schematic diagram of the aerodynamic power measurement system. The dynamic pressure (h_d) at the center of the inlet duct and the suction pressure (h_s) at the vacuum chamber were measured using a micromanometer. These two pressures were used to calculate the aerodynamic power of the vacuum cleaner.

The aerodynamic power (AP) is defined as the net time rate of work done by the vacuum cleaner while expending energy to produce the suction

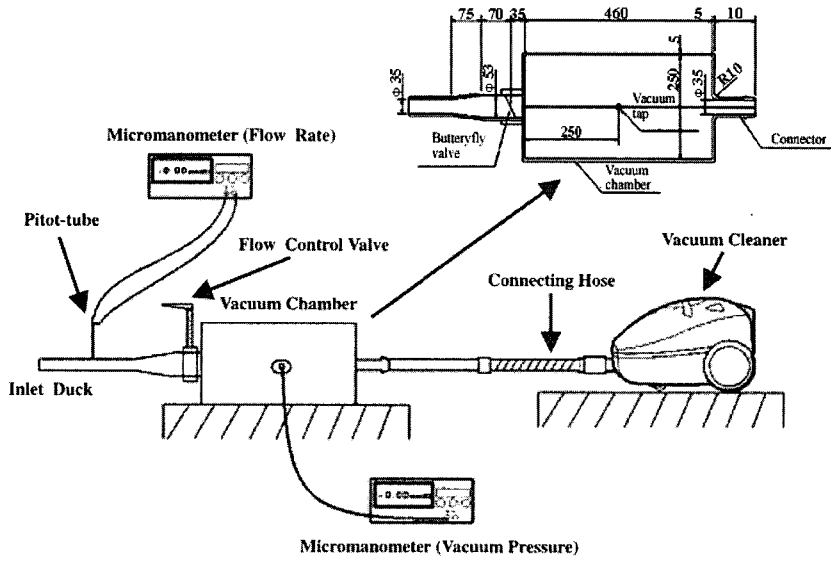


Fig. 5 Experimental set-up for aerodynamic power measurement

air under a specified air resistance condition. By applying Bernoulli’s equation and momentum conservation law, we can get the aerodynamic power (Park and Lee, 2004)

$$\begin{aligned} AP &= 0.1633 \times Q \times h_s \\ &= 3.1027 \times 10^{-2} \times \sqrt{h_d} \times h_s \end{aligned} \quad (1)$$

where AP is the aerodynamic power in watts (W), Q is the flow rate (m^3/min), and h_s is the suction pressure in absolute vacuum pressure (mmH_2O). By measuring the suction pressure h_s and dynamic pressure h_d of air stream, we evaluated the aerodynamic power of each vacuum cleaner with different intake head. The suction efficiency η is defined as the ratio of the maximum aerodynamic power (AP_{max}) of an intake head to the maximum aerodynamic power without the intake head (AP_{mo}).

$$\eta = AP_{max} / AP_{mo} \quad (2)$$

The noise level of the vacuum cleaner was measured in an anechoic chamber using a microphone sound level meter. The test methods for the aerodynamic power and noise level measurements were described in detail in Park and Lee (2004).

3. Results and Discussion

3.1 Flow visualization of intake heads tested

Fig. 6 show typical visualized flow images for the original intake head to demonstrate the sucking process of particles in sequence. The flow images show the movement of collecting dust particles into the suction hole of the intake head. It takes about 280 ms for the flow field, i.e. tracing particle movements, to become a steady state from the start. The time interval between sequent flow images shown in Fig. 6 is 48 ms. At the initial stage, the vertical flow motion is dominant and the particles move upward from lower side of the suction hole at the elapse time of $\tau=40$ ms. However, the particles sucking from the horizontal side trenches are difficult to figure out and the particle movement in the horizontal trenches is enhanced gradually. At the junction of suction hole and trenches, the upward flow motion from the lower side is disturbed by the horizontal flow from the side trenches shown at the elapse time of $\tau=88$ ms. With further development of sucking flow, the upward moving flow from the lower side and the flows from the side trenches impinge at the entrance of suction nozzle. The particles

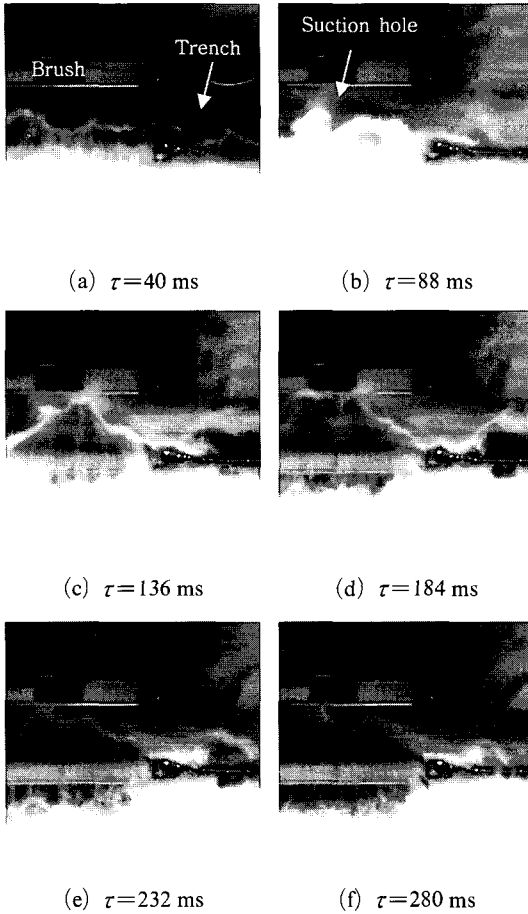


Fig. 6 Evolution of flow field at the original intake head

moving in vertical direction are suppressed by the horizontal flows from both side trenches. In consequence, the uprising particles form a triangle shape in the central suction area as shown in Fig. 6(c). The side edges of the triangle are formed by the impact of particles moving in both vertical and horizontal directions. Some particles moving downward from the upper side form another triangle in an upside down shape at the upper corners of the central suction area. Subsequently, the converging flow from the horizontal and vertical directions starts to approach an equilibrium state and side angles of the triangles keep 40° at $\tau=184$ ms. The particles located above the right trench are entrained into the suction hole due to rapid horizontal flow ($\tau=232$ ms). Finally, the particle motion reaches a steady

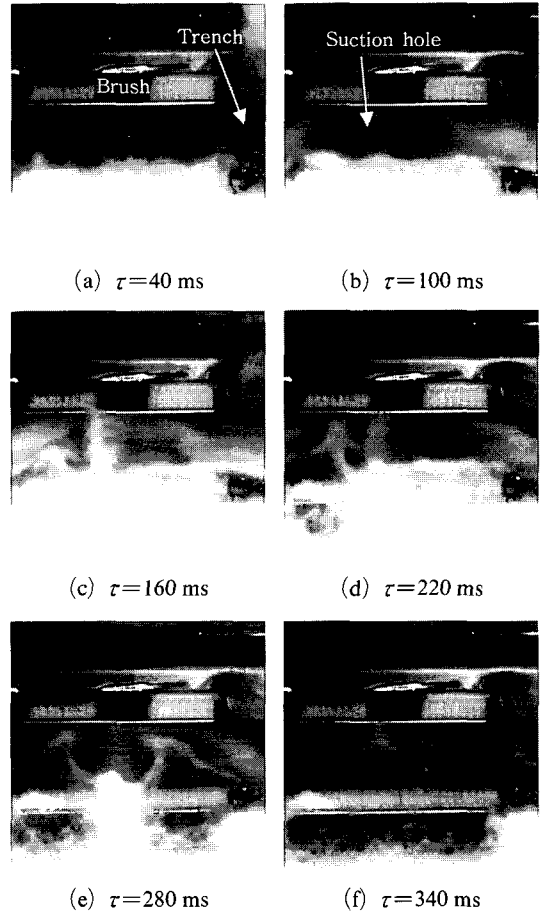


Fig. 7 Evolution of flow field for intake head modified in a contraction chamber

state at the elapse time of $\tau=280$ ms.

The temporal evolution of particle entrainment for the intake head modified in the contraction chamber is shown in Fig. 7. It takes about 340 ms from the start to the steady state of particle movement. The elapse time is longer than the 280 ms for the original intake head. This implies that the dust-collecting ability of the modified model is lower than that of the original one. At the initial stage, the particles moving downward from the upper side of the suction hole is dominant and it suppresses the upward flow moving from the lower side of suction hole ($\tau=40$ ms). However, the horizontal moving flow from two side trenches become stronger compared with that of original intake head. They collide each other at the central region of the

suction hole at $\tau=100$ ms. Thereafter, the particle motion in vertical direction is enhanced, some particles located near lower side of the suction hole near the trench are entrained by the suction flow from left trench and form a small vortex as shown in Fig. 7(c) at $\tau=160$ ms. This flow pattern lasts for a relatively long period of time until $\tau=220$ ms. As the elapse time increases, more and more particles are collected from the lower side of the suction hole. However, the upward moving flow at the central part is still suppressed by the strong intake flow from the upper side, leading to form two vortices at the entrance of suction hole, shown in Fig. 7(e) at $\tau=280$ ms. The flows in the vertical and horizontal directions reach a balance gradually and the symmetric vortices finally disappear at $\tau=340$ ms.

Fig. 8 shows the typical instantaneous particle motion with flow for the intake head modified in both of connection chamber and trench height. The general behavior of flow evolution is similar to that of intake head modified in contraction chamber. However, the elapsed time between the starting and the final steady state of flow motion is about 320 ms. It is a little bit shorter than that of a connection chamber modified model. At the initial stage, the flow in vertical direction is weak and a swarm of particles moved from the side trenches is entrained into the suction hole. However, small number of particles is sucked from the lower side of the suction hole ($\tau=40$ –96 ms). At elapse time of $\tau=152$ ms, the entrainment of particles from the lower side starts to increase with the enhancement of vertical suction flow. Two vortices are also formed by the interaction of flows from the vertical and horizontal directions at $\tau=208$ ms and $\tau=264$ ms. The vortices disappear quickly and finally the flow field reaches a steady state in the suction hole ($\tau=320$ ms).

From the flow visualization results, we can conjecture briefly that the suction efficiency for the intake head modified in both of the connection chamber and trench height is lower than that of the original intake head. However, the improvement of efficiency and acoustic noise

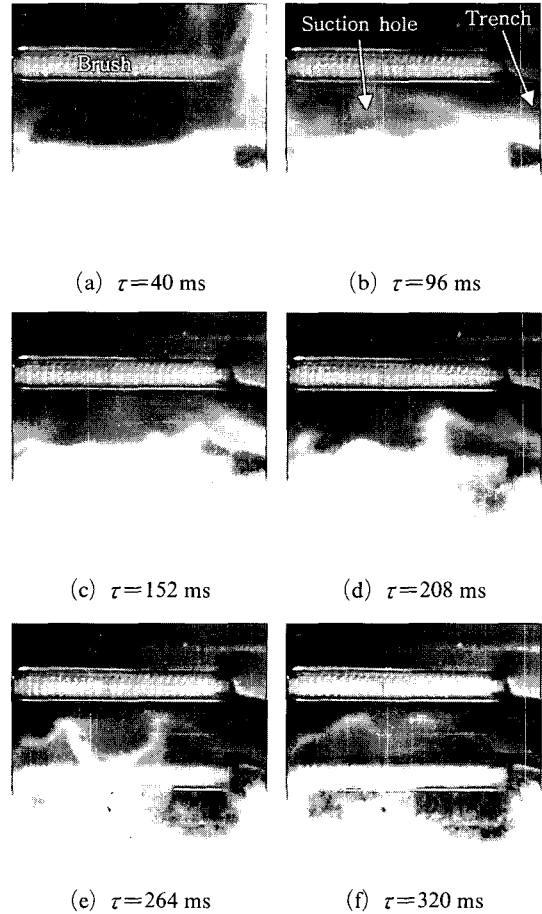
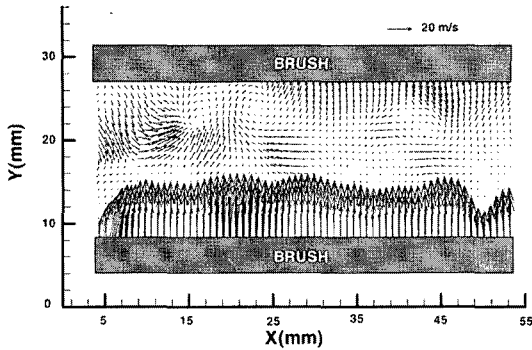


Fig. 8 Evolution of flow field for intake head modified in both connection chamber and trench height

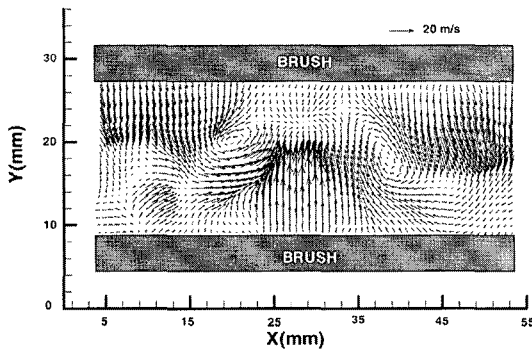
level by the intake head modification in steady state will be discussed later.

3.2 Velocity field measurement

Typical instantaneous velocity fields measured at the starting stage and steady state for the original intake head are shown in Fig. 9. At the initial stage, the flow moving upward from lower side of the suction hole has high speed as shown in Fig. 9(a). The maximum vertical flow speed (Y-directional, the coordinate system is defined in Fig. 4) is about $V_{\max}=50.87$ m/s, but the maximum horizontal (X-directional) velocity is only $U_{\max}=6.94$ m/s. This indicates that the dust collection ability from side trenches is very weak at the starting stage. In addition, due to initial



(a) Initial stage

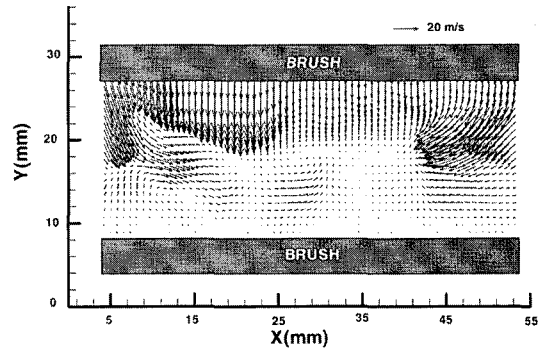


(b) Steady state

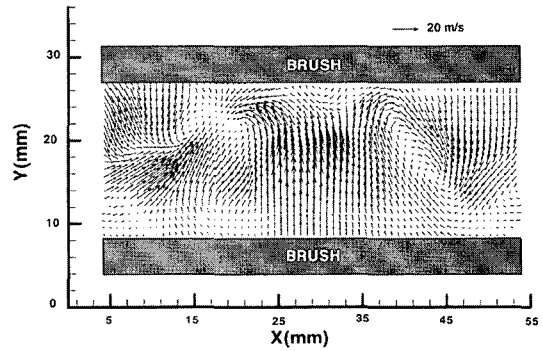
Fig. 9 Instantaneous velocity field for original intake head

instability of the flow stream, the flow at the entrance region of the suction hole shows relatively strong turbulence and asymmetric flow pattern.

After the flow field reaches a steady state, the flow moving downward from upper side of the suction hole is enhanced, suppressing the upward moving flow from the lower side and decreasing its speed. Though the vertical flow motion is still strong, the maximum vertical flow velocity is decreased to $V_{max}=43.61$ m/s, and the horizontal velocity is increased to $U_{max}=10.59$ m/s, about 25% of the vertical flow speed. In the region near the upper and lower sides of the intake head, the velocity field is nearly symmetric with respect to the vertical centerline. At the left and right sides of suction hole, the flow from the upper part of trench moves downward at high speed, however, the speed of downward moving flow is very slow at the up-center area of the suction hole. On the other hand, the flow moving



(a) Initial stage



(b) Steady state

Fig. 10 Instantaneous velocity field for intake head modified in the connection chamber

upward from the lower side has maximum speed at the center region. The vertical and horizontal directional flows interact at the entrance of the suction hole and form a triangular flow patten. The combined flows are sucked into the hole with generating two large-scale vortices.

Fig. 10 shows the instantaneous velocity fields for the intake head modified in the connection chamber at the starting stage and the steady state. At the starting stage, the general flow structure is quite different from that of the original intake head. The flow moving downward has higher speed, and the horizontal flow at both upper corners of the suction hole is also strong. The combined flow converges to the center of suction hole with suppressing the flow moving upward from the lower side of the suction hole. The horizontal flow velocity is increased significantly, compared with that of original intake head. At the initial stage, the maximum horizontal and vertical flow speed are $U_{max}=13.18$ m/s,

and $V_{\max}=34.65$ m/s, respectively. Afterward, the flow from the lower side of the suction hole is enhanced gradually, and when flow field reaches a steady state, the upward moving flow becomes dominant at the central region. At the steady state, the general flow structure is similar to that of the original intake head. In the region where the upward and downward flows meet each other, two large vortices are formed and the velocity field is also nearly symmetric. However, the maximum vertical flow velocity is $V_{\max}=33.83$ m/s, less than that of the original intake head. On the other hand, the maximum horizontal flow velocity is increased to $U_{\max}=14.33$ m/s, about 44% of V_{\max} . This implies that the dust-collection ability along the side trenches is improved at the expense of suction ability in the vertical direction.

Figure 11 shows the instantaneous velocity fields for the intake head modified both the trench height and the connection chamber. In this case, the horizontal flow along the side trenches is dominant at the starting stage as shown in Fig. 11(a). The vertical flow from upper and lower sides of the suction hole is relatively weak. The horizontal flow motion is much stronger than the former two cases, the maximum flow speed is $U_{\max}=17.09$ m/s. This seems to result from the improvement of flow resistance due to reduction of flow separation and turbulence by decreasing the slope of the side trenches. Direct impingement of the flows from two side trenches leads to several small-scale vortices and causes asymmetric flow structure in the entrance region of the suction hole.

As the flow becomes a steady state, the flow moving upward is enhanced significantly, the maximum vertical flow speed is about $V_{\max}=31.35$ m/s, and the maximum magnitude of horizontal velocity component maintains the same level as the horizontal velocity at initial stage. Compared with the original intake head, the upward moving flow region is wider. The downward flow from the upper side is relatively weak. The ratio of U_{\max} to V_{\max} is increased up to 55%; the dust-collection ability from side trenches is further improved. The vortex structure formed

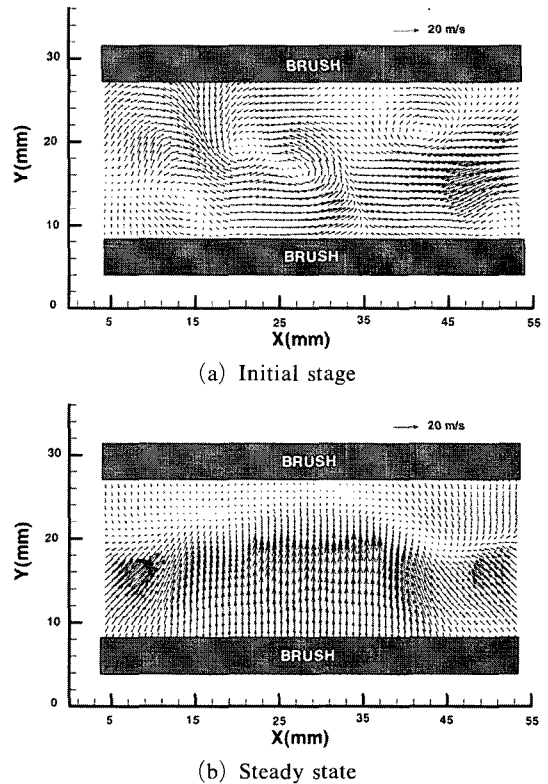


Fig. 11 Instantaneous velocity field for intake head modified in both connection chamber and trench height

at the suction hole is not so clear compared with the other two cases.

3.3 Aerodynamic power, suction efficiency and noise level

To evaluate the performance of the vacuum cleaner with different intake heads, the aerodynamic power of vacuum cleaner was measured. Fig. 12 represents the comparison of aerodynamic powers of different intake head modifications. Each intake head was fixed over the artificial lawn to simulate the surface condition of carpet. The aerodynamic power has a parabolic distribution as a function of airflow rate. It increases up to the maximum at small flow rate and then decreases on further increase of the airflow rate. The vacuum cleaner without any intake head has the maximum aerodynamic power at the flow rate of $Q=1.23$ m³/min due to minimization of momentum loss in the suction process, in this

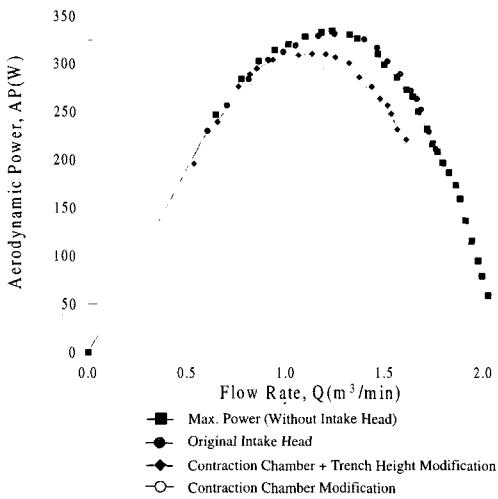


Fig. 12 Comparison of aerodynamic power

case, we assume that the suction efficiency is 100%.

The aerodynamic power and suction efficiency of the vacuum cleaner with the original intake head are similar to those of vacuum cleaner without the intake head. When the connection chamber was modified, the aerodynamic power is decreased remarkably and the suction efficiency is about 90% of that for the vacuum cleaner without intake head. The decreasing of suction efficiency can be confirmed by the longer elapse time of flow field from the start to a steady state as mentioned in the flow visualization results. For the intake head modified both the connection chamber and trench height, the aerodynamic power lays between the values of the original intake head and the intake head modified only in the connection chamber, and the suction efficiency is increased to 93%.

Considering the noise level is another important parameter to evaluate the quality of a vacuum cleaner. Though the modification to the intake head decreases the aerodynamic power and suction efficiency, the acoustic noise level is also decreased for both modifications as summarized in Table 1. For the combined modification on the contraction chamber and trench height, the noise level was reduced about 3.338dB compared with that of original intake head. However, it is less than the noise level reduction of intake head

Table 1 Comparison of suction efficiency and noise level of intake heads tested

Intake Head Modification	Suction Efficiency	Noise Level (dB)	Noise Level Reduction (dB)
Original Intake Head	99%	72.175	0
Chamber Contraction	90%	67.812	-4.363
Trench Height + Chamber Contraction	93%	68.837	-3.338

modified with a contraction chamber only, but it has better suction efficiency and aerodynamic power. Therefore, the intake head modified both the connection chamber and trench height can be considered as a compromising design in view points of suction efficiency and acoustic characteristic.

4. Conclusions

Flow fields at the entrance region of intake heads of a commercial vacuum cleaner were investigated using flow visualization and PIV techniques. The aerodynamic power, suction efficiency and noise level of the intake heads were also measured. In order to investigate the dust-collection ability and acoustic characteristic, the internal structure of an intake head was modified by varying the slope of bottom surface of side trench height and connection chamber, respectively. The flow fields of the original intake head and modified types were compared in this study. The original intake head shows a powerful suction ability in collecting dusts, and the flow field gets to a steady state in a shorter elapse time, compared with two other modified intake heads.

When a smooth contraction surface was employed inside the connection chamber, the vertical flow speed is decreased with the increase of horizontal flow velocity. The strength of two vortices sucking into the suction hole is weaker compared with the original intake head. When the trench height is modified together with the contraction chamber, the reduced slope of side

trench influences the flow structure and increase the horizontal flow velocity. With decreasing of the vertical flow velocity, the dust-collection ability in Y directions is enhanced.

From the viewpoint of aerodynamic power and suction efficiency, the effect of flow path modifications on the dust-collection ability was found to be slightly negative in this study. However, the aero-acoustic noise level was reduced notably and it deserves well of keeping balance of intake head performance in X and Y directions. The combined modification on the connection chamber and trench height can be considered as a compromised design candidate to reduce the aero-acoustic noise caused by flow separation in the intake head.

Acknowledgments

This work was supported in part by LG electronic company and NRL (National Research Laboratory) program of the Ministry of Science and Technology, Korea.

References

- Bentouati, S., Zhu, Z. Q. and Howe, D., 1999, "Permanent Magnet Brushless DC Motors for Consumer Products," *Proc. 9th International Conference on Electrical Machines and Drives*, pp. 118~122.
- Brungart, T. A. and Lauchle, G. C., 2001, "Modifications of a Handheld Vacuum Cleaner for Noise Control," *Journal of Noise Control Engineering*, Vol. 49, pp. 73~78.
- Omori, M. and Uzawa, H., 1997, "Brush Vacuum Cleaner," *Japan TAPPI Journal*, Vol. 51, No. 2, pp. 76~79.
- Park, C. W., Lee, S. I. and Lee, S. J., 2004, "Experimental Investigation on the Reduction of Aero-acoustic Noise of Vacuum Cleaner Suction Nozzle," *KSME International Journal*, accepted, in press.
- Raffel, M., Willert, C. and Kompenhans, J., 1998, *Particle Image Velocimetry*, ISBN 3-540-63683-8, Springer.
- Sarbu, M. and Kraft, G., 1996, "Sound Intensity Techniques Reduce Vacuum Cleaner Noise," *Noise and Vibration Worldwide*, Vol. 27, pp. 10~14.
- Tuncay, R. N., Yilmaz, M. and Onculoglu, C., 2001, "The Design Methodology to Develop New-Generation Universal-Motors for Vacuum Cleaners," *Proc. IEEE International Conference on Electrical Machines and Drives*, pp. 926~930.